

# Direct Synthesis of Metal Cluster Complexes by Deposition of Mass-Selected Clusters with Ligand: Iron with CO

S. Fedrigo, T. L. Haslett, and M. Moskovits\*

Contribution from the Department of Chemistry, University of Toronto and Ontario Laser and Lightwave Research Centre, Toronto, Canada M5S 1A1

Received December 19, 1995<sup>⊗</sup>

**Abstract:** A new technique for preparing metal cluster complexes of a desired nuclearity by co-depositing ligand with metal clusters mass-selected from a cluster beam is illustrated by the deposition of Fe, Fe<sub>2</sub>, and Fe<sub>3</sub> with excess CO. The matrices formed were studied by Fourier transform infrared spectroscopy. Unexpectedly, deposition of Fe<sub>2</sub> produced the CO-unbridged Fe<sub>2</sub>(CO)<sub>8</sub> isomer, known primarily from matrix photochemistry, rather than the well-known diiron nonacarbonyl.

Many hundreds of transition-metal cluster complexes have been synthesized, in part in the search for novel homogeneous catalysts.<sup>1</sup> Some have been used as models for adsorbed species and heterogeneous bulk metal catalysts.<sup>2</sup> Among the latter, the carbonyl complexes occupy a significant place due to the importance of CO as an adsorbate and the prominence of CO reduction among reactions involving heterogeneous catalysts. A large number of both mononuclear and polynuclear metal cluster binary carbonyls are known.<sup>2,3</sup> However, one suspects that a significant number of polynuclear metal carbonyls remain to be discovered. Most metal carbonyls are prepared from the mononuclear precursor under reductive conditions.<sup>4</sup> Exceptions are the Fe<sub>2</sub>, Ru<sub>2</sub>, and Os<sub>2</sub> carbonyls, which are produced photochemically.<sup>5</sup> In a few cases, polynuclear metal carbonyls were formed in low-temperature matrices by co-condensing the metal atom vapor with a CO-doped matrix gas at high metal/gas ratio.<sup>6</sup> The co-condensation of metal with ligand at low temperatures is also the strategy behind metal-vapor synthesis.<sup>7</sup> Useful products were obtained using this technique by purifying the very large assortment of products formed.

In this paper, we report a new technique for directly synthesizing polynuclear metal complexes in sufficient quantities to record their IR spectra by co-depositing excess ligand with size-selected metal cluster ions from a metal cluster beam onto a cold substrate. The process is illustrated with iron clusters and CO. The infrared absorption spectra in the CO vibration region of iron atom, dimer, and trimer carbonyls are presented and compared to known Fe<sub>n</sub>(CO)<sub>y</sub> spectra. Deposits of Fe<sup>+</sup> and Fe<sub>3</sub><sup>+</sup> produce predominantly the well-known Fe(CO)<sub>5</sub> and Fe<sub>3</sub>(CO)<sub>12</sub> species. However, the major fraction of the dimer carbonyl produced by the deposition of Fe<sub>2</sub><sup>+</sup> in CO is the unbridged isomer of Fe<sub>2</sub>(CO)<sub>8</sub>, which was observed previously

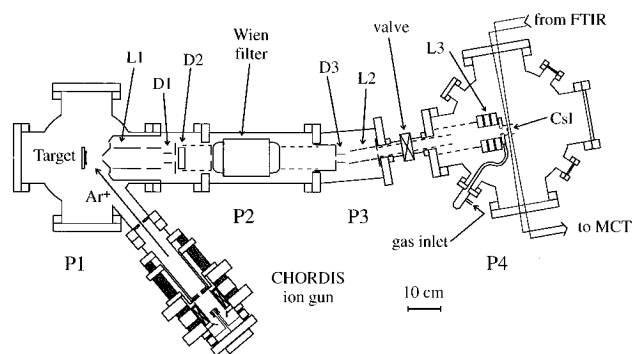


**Figure 1.** Experimental apparatus. P1, P2, P3, and P4 represent separately pumped vacuum stages. During deposition, P1 is at  $4 \times 10^{-6}$  Torr, while P4 remains at  $8 \times 10^{-10}$  Torr with no matrix gas load. L = ion lens; D = deflection plates.

only after photolysis of the more usual diiron carbonyl Fe<sub>2</sub>(CO)<sub>9</sub>, which produces the bridged form of Fe<sub>2</sub>(CO)<sub>8</sub> as an intermediate.<sup>8</sup>

## Experimental Section

The experimental apparatus (Figure 1) has been described previously.<sup>9</sup> Briefly, iron cluster ions were produced by high-voltage sputtering an Fe target (Aldrich, purity 99.9%), mass-selected using a Wien filter, and co-deposited with carbon monoxide (Matheson, purity 99.99%) on a cold cesium iodide window (25 K). Ions were neutralized with a low-energy electron beam situated in the deposition area; however, it is unclear whether the neutralization occurs before, during, or after the cluster-CO reaction. CO was introduced into the deposition chamber through a leak valve. Commercial CO contains traces of residual Ni carbonyl, which was largely removed by a liquid N<sub>2</sub> trap. The pressure in the deposition chamber was  $6 \times 10^{-10}$  Torr with the sample cold, rising to  $8 \times 10^{-10}$  Torr during the deposition when no CO was injected. The currents and the mean kinetic energies of the iron atomic, diatomic and triatomic beams during the deposition were respectively 13 nA/20 eV, 7 nA/20 eV and 2 nA/25 eV. Currents were measured on an 8 mm wide plate. Absorption spectra were collected by passing the modulated beam of a 1 cm<sup>-1</sup> resolution Fourier transform infrared spectrometer (Bomem MB-100) through the sample onto an MCT detector. The infrared beam was focused at the sample by a 35 cm focal length mirror, passing through a 3 × 8 mm slit 4 mm in front of the sample. By translating the sample, the absorption could be measured as a function of the vertical position across the deposit. Peaks

(8) Poliakoff, M.; Turner, J. J. *J. Chem. Soc. (A)* **1971**, 2403–2410.

(9) Haslett, T. L.; Fedrigo, S.; Moskovits, M. *J. Chem. Phys.* **1995**, *103*, 7815–7819.

<sup>⊗</sup> Abstract published in *Advance ACS Abstracts*, May 1, 1996.

(1) (a) Parshall, G. W.; Ittel, S. D. *Homogeneous Catalysis*, 2nd ed.; Wiley: New York, 1992. (b) Süß-Fink, G.; Meister, G. *Advances in Organometallic Chemistry*; Stone, F. G. A., West, R., Eds.; Academic Press: San Diego, 1993; Vol. 35.

(2) Muetterties, E. L.; Rhodin, T. N.; Band, E.; Brucker, C. F.; Pretzer, W. R. *Chem. Rev.* **1979**, *79*, 91–137.

(3) Moskovits, M.; Ozin, G. A. *Cryochemistry*; Moskovits, M., Ozin, G. A., Eds.; Wiley: New York, 1976; pp 395–439.

(4) Cotton, F. A.; Wilkinson, G. *Advanced Inorganic Chemistry*; Wiley: New York, 1980.

(5) Wrighton, M. *Chem. Rev.* **1974**, *74*, 401–430.

(6) Peden, C. H. F.; Parker, S. F.; Barret, P. H.; Pearson, R. G. *J. Phys. Chem.* **1983**, *87*, 2329–2336.

(7) (a) Timms, P. L. *Proc. R. Soc. London, Ser. A* **1984**, *396*, 1. (b) Green, M. L. H. *J. Organomet. Chem.* **1980**, *200*, 119.

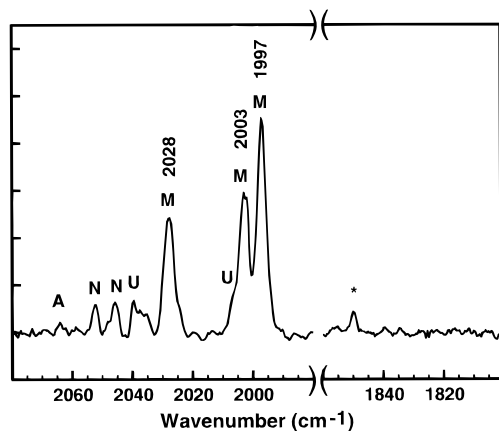


**Figure 2.** Infrared absorbance spectrum of iron atoms deposited in CO matrix. A base line is subtracted. The strongest peak corresponds to an absorbance of 0.005. The labels correspond to the center frequencies and assignments of the infrared absorbance peaks obtained by a multi-Gaussian fit of the spectrum. M =  $\text{Fe}(\text{CO})_5$ , U = unbridged  $\text{Fe}_2(\text{CO})_8$ , N =  $\text{Ni}(\text{CO})_4$ , A =  $\text{Fe}_2(\text{CO})_9$ . The peak marked with an asterisk is unknown; possibly  $\text{Fe}(\text{CO})_4^-$ .

whose intensities correlated with the beam profile were assumed to be related to species originating in the cluster beam. The spatial profile of the cluster ion beam was roughly Gaussian, with a full width at half maximum of approximately 5 mm. The CO:metal ratio was approximately 10<sup>4</sup>:1 in all cases.

## Results and Discussion

The IR spectrum obtained after the deposition of  $9 \times 10^{14}$   $\text{cm}^{-2}$  of  $\text{Fe}^+$  shows three strong absorption peaks centered at 2028, 2003, and 1997  $\text{cm}^{-1}$  (Figure 2). They are assigned to trigonal bipyramidal  $\text{Fe}(\text{CO})_5$ , which has IR-active  $A_2''$  and  $E'$  modes.<sup>10</sup> The 2028- $\text{cm}^{-1}$  band is assigned to the  $A_2''$  mode while the two lower frequencies belong to the  $E'$  mode, which is split. The band split is induced by the interaction between the iron carbonyl and the matrix, and could be due either to a distortion of the molecule or to the fact that the carbonyl may be trapped in different matrix sites.<sup>10</sup> Except for one unknown band at 1850  $\text{cm}^{-1}$ , all other bands are assigned to  $\text{Ni}(\text{CO})_4$  (again, a split band), which is present as an impurity in the CO gas, and  $\text{Fe}_2$  carbonyls.  $\text{Fe}_2^+$  is virtually non-existent in the beam, therefore the small quantity of diiron carbonyl is due to atom diffusion in the freshly formed matrix—an effect previously exploited in matrix isolation experiments to form aggregates.<sup>11</sup> A great deal of energy is available to aid the diffusion process including the neutralization energy of the cations, the exoergicity of the Fe carbonylation, and the deposition kinetic energy. The band at 1850  $\text{cm}^{-1}$  is possibly due to  $\text{Fe}(\text{CO})_4^-$ . A frequency of 1854  $\text{cm}^{-1}$  was reported for that anion by Breeze et al.<sup>12</sup> In any case, the band intensity correlates with the beam profile.

For clarity of detail, the spectra presented are divided into two regions: the region between 2080 and 1980  $\text{cm}^{-1}$  encompasses vibrational modes of terminally-bonded CO ligands while the 1900–1800- $\text{cm}^{-1}$  region contains modes of CO ligands bridge-bonded to two Fe atoms. No bands were observed between these regions. The full width at half maximum of a single absorption band is approximately 4  $\text{cm}^{-1}$  in all the spectra presented. This is more than five times the width observed in

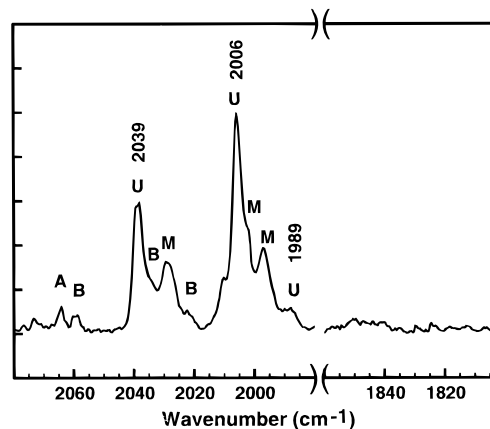


**Figure 3.** Infrared absorbance spectrum of iron dimers deposited in CO matrix. A base line is subtracted. The strongest peak corresponds to an absorbance of 0.01. U = unbridged  $\text{Fe}_2(\text{CO})_8$ , M =  $\text{Fe}(\text{CO})_5$ , A =  $\text{Fe}_2(\text{CO})_9$ , B = bridged  $\text{Fe}_2(\text{CO})_8$ .

the spectra of iron carbonyls deposited in argon matrices.<sup>13</sup> The broadening is not due to spectrometer resolution, as the isotopic CO peaks are observed to have widths of 1  $\text{cm}^{-1}$ , but rather may be due to the fact that the carbonyls are isolated in a solid CO matrix.

The IR spectrum obtained after depositing  $1.2 \times 10^{15}$   $\text{cm}^{-2}$  of  $\text{Fe}_2^+$  with CO is shown in Figure 3. Several absorptions are observed in the terminal region. The medium intensity peaks centered at 2028.5 and 1997  $\text{cm}^{-1}$  are clearly the fingerprint of the  $\text{Fe}(\text{CO})_5$  species. This is likely due to fragmentation of the iron dimers during deposition. However, although the 20 eV mean kinetic energy of the ion beam greatly exceeds the diiron bond energy (1.15 eV) or the bond energies of  $\text{Fe}_2^+$  and  $\text{Fe}_3^+$ ,<sup>14</sup> less than 30% of the dimers fragment (based on an analysis of the band areas, assuming roughly equal transition dipole values for the CO's, as well as on a determination of the absolute  $\text{Fe}(\text{CO})_5$  band intensities in the  $\text{Fe}_2^+$  matrices as compared to the intensities observed for the pentacarbonyl in  $\text{Fe}^+$  deposits of known total metal content). This is undoubtedly due to energy dissipation by collision with CO molecules in the surface region of the solid CO film and has been reported and calculated.<sup>15,16</sup> On the basis of the work of Poliakoff and co-workers,<sup>8</sup> all of the other bands can be assigned to  $\text{Fe}_2(\text{CO})_9$ ,  $\text{Fe}_2(\text{CO})_8$  having two bridging CO's (form B), and  $\text{Fe}_2(\text{CO})_8$  in which all the CO's are terminally bonded (form U).  $\text{Fe}_2(\text{CO})_9$  has  $D_{3h}$  symmetry, while the structures of the B and U forms of  $\text{Fe}_2(\text{CO})_8$  have been deduced to be  $C_{2v}$  and  $D_{2h}$ , respectively.<sup>17</sup> The major product in the deposit is the unbridged form of  $\text{Fe}_2(\text{CO})_8$  (U), identified by the two strong peaks centered at 2039 and 2006  $\text{cm}^{-1}$ . The dimer carbonyl formed in the photoreaction of  $\text{Fe}(\text{CO})_5$  is exclusively  $\text{Fe}_2(\text{CO})_9$ , which has three bridging CO's,<sup>8</sup> while the unbridged form of  $\text{Fe}_2(\text{CO})_8$  can only be obtained after UV/visible photolysis of  $\text{Fe}_2(\text{CO})_9$ . The bridged form of the octacarbonyl was observed as an intermediate.<sup>8</sup>  $\text{Fe}_2(\text{CO})_9$  and B are also present in our sample in small quantities. We estimate that they correspond to less than 5% of the diiron

(13) Poliakoff, M. *Chem. Phys. Lett.* **1981**, 78, 1–3.

(14) Loh, S. K.; Lian, L.; Hales, D. A.; Armentrout, P. B. *J. Phys. Chem.* **1988**, 92, 4009–4012. Loh, S. K.; Hales, D. A.; Lian, L.; Armentrout, P. B. *J. Chem. Phys.* **1989**, 90, 5466. Lian, L.; Su, C.-X.; Armentrout, P. B. *J. Chem. Phys.* **1992**, 97, 4072.

(15) Harbich, W.; Fedrigo, S.; Meyer, F.; Lindsay, D. M.; Lignieres, J.; Rivoal, J. C.; Kreisler, D. *J. Chem. Phys.* **1990**, 93, 8535–8543. Hu, Z.; Shen, B.; Zhou, Q.; Desaran, S.; Lombardi, J. R.; Harbich, W.; Lindsay, D. M. *J. Chem. Phys.* **1991**, 95, 2206–2209.

(16) Cheng, H. P.; Landman, U. *Science* **1993**, 260, 1304–1307.

(17) Fletcher, S. C.; Poliakoff, M.; Turner, J. J. *Inorg. Chem.* **1986**, 25, 3597–3604.

(10) Poliakoff, M.; Turner, J. J. *J. Chem. Soc., Dalton Trans.* **1973**, 13, 1351–1357.

(11) Moskovits, M.; Hulse, J. E. *J. Chem. Soc., Faraday Trans.* **1977**, 73, 471–484.

(12) Breeze, P. A.; Burdett, J. K.; Turner, J. J. *Inorg. Chem.* **1981**, 20, 3369–3378.

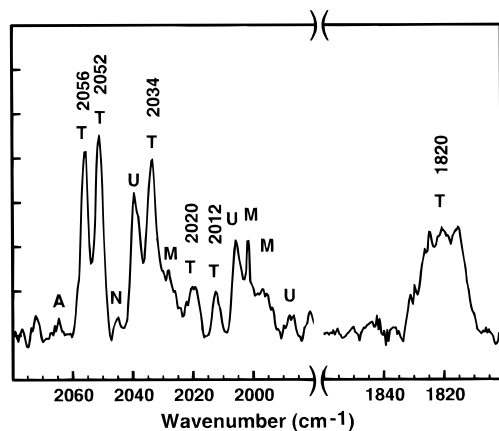


**Figure 4.** Infrared absorbance spectrum of iron trimers deposited in CO matrix. A base line is subtracted. The strongest peak corresponds to an absorbance of 0.002. T =  $\text{Fe}_3(\text{CO})_{12}$ , U = unbridged  $\text{Fe}_2(\text{CO})_8$ , M =  $\text{Fe}(\text{CO})_5$ , A =  $\text{Fe}_2(\text{CO})_9$ , N =  $\text{Ni}(\text{CO})_4$ .

species in the matrix. Species U remained the predominant molecule in the matrix even after annealing to 50 K, indicating that the species is stable to at least this temperature. This agrees with the report of Poliakoff and co-workers, who showed that the quantity of the unbridged isomer increased during successive cycles of photolysis and annealing.<sup>8</sup> The same authors also demonstrated that B transforms to  $\text{Fe}_2(\text{CO})_9$  and to U upon annealing, the branching ratio being determined by the concentration of CO in the matrix. When CO is in excess it preferentially produces the nonacarbonyl. Our samples were not exposed to UV or visible light from any source—including the IR source—hence we conclude that  $\text{Fe}_2(\text{CO})_8$  (U form) is formed directly in the reaction of  $\text{Fe}_2$  with CO and that it is the major product of that reaction. It is not known if the  $\text{Fe}_2$  is ionic during the reaction.

Figure 4 shows the IR spectrum obtained following the co-deposition of  $4 \times 10^{14} \text{ cm}^{-2}$  of  $\text{Fe}_3^+$  with CO. The major features centered at 2056, 2051, and 2034  $\text{cm}^{-1}$  correspond well to the IR peaks reported by Poliakoff and Turner for the  $\text{C}_{2v}$  form of  $\text{Fe}_3(\text{CO})_{12}$  deposited in matrices of argon (2056, 2051, and 2036  $\text{cm}^{-1}$ ) and nitrogen (2058, 2053, and 2036  $\text{cm}^{-1}$ ).<sup>18</sup> We can, therefore, conclude confidently that the major product formed by co-depositing  $\text{Fe}_3^+$  with CO is the known triiron dodecacarbonyl. The bands at 2020 and 2012  $\text{cm}^{-1}$  as well as the broad feature centered near 1820  $\text{cm}^{-1}$  in the bridging region also belong to this species.<sup>18</sup> The main discrepancies with the previous matrix isolation spectra are the bridging frequency (1820  $\text{cm}^{-1}$  versus 1828  $\text{cm}^{-1}$  in  $\text{N}_2$  and 1833  $\text{cm}^{-1}$  in Ar) and the bridging intensity relative to the terminal bands, which is not surprising given the known sensitivity of the bridging carbonyl groups to their environment.<sup>18</sup> The weak features at 2002 and 1997.5  $\text{cm}^{-1}$  correspond to  $\text{Fe}(\text{CO})_5$ . The bands at 2039 and 2005.5  $\text{cm}^{-1}$  are attributable to the unbridged isomer of  $\text{Fe}_2(\text{CO})_8$ . Finally, the weak peak at 2065  $\text{cm}^{-1}$  corresponds to the strongest absorption of  $\text{Fe}_2(\text{CO})_9$ . Here, again we ascribe the presence of the small quantities of mono- and diiron species to fragmentation of the triiron during deposition. The fragmentation products account for less than 25% of the iron in the matrix. Interestingly, the diiron carbonyls formed due to the fragmentation of the triiron maintain roughly the same product ratios as when  $\text{Fe}_2^+$  is directly deposited.

The formation of  $\text{Fe}(\text{CO})_5$  by co-condensing Fe atoms with CO is not surprising. In contrast, the formation of  $\text{Fe}_2(\text{CO})_8$ , rather than the commonly encountered  $\text{Fe}_2(\text{CO})_9$ , when  $\text{Fe}_2$  is co-deposited with CO is surprising, although there is no *a priori*

reason why the two synthetic routes should lead to the same product. In fact, it is not known unequivocally that the nonacarbonyl is the more stable of the two species, although, based on the fact that the nonacarbonyl is the major product formed in the photodimerization of  $\text{Fe}(\text{CO})_5$ , one might suspect it to be so. Even if species U is less stable than the nonacarbonyl, it may be metastable under the conditions of its formation. One might conjecture that this metastability is related to the absence of a true metal–metal bond in the nonacarbonyl, which implies that forming the nonacarbonyl from the naked iron dimer precursor would entail breaking the iron–iron bond, which may involve overcoming an energy barrier. Recent calculations suggest that there is no direct Fe–Fe bond in  $\text{Fe}_2(\text{CO})_9$ ,<sup>19</sup> i.e. the bi-octahedron is linked exclusively through the CO-bridge bonds. In contrast, a double bond is expected between the iron atoms of the unbridged  $\text{Fe}_2(\text{CO})_8$ , not unlike the bonding in  $\text{Fe}_2$ . The iron–iron distance in the nonacarbonyl is 2.52 Å,<sup>20</sup> while in the iron dimer it is only 2.02 Å.<sup>21</sup> One might then speculate that an energy barrier associated with the Fe–Fe bond extension separates the nonacarbonyl from its  $\text{Fe}_2/\text{CO}$  precursors, but this seems unlikely given that the metal–metal distances in bridged carbonyls are generally found to be from 0.03 to 0.1 Å shorter than in unbridged species.<sup>2</sup> Hence, although the Fe–Fe distance in unbridged  $\text{Fe}_2(\text{CO})_8$  is unknown, we would expect its value to be comparable to that found in the nonacarbonyl. It seems more likely that any energy barrier might more properly be linked to the extensive rearrangement in the electronic character of the Fe–Fe bonding—a barrier that would not exist for the  $\text{Fe}(\text{CO})_5$  precursor.

The species  $\text{Fe}_3(\text{CO})_{12}$  that is produced from  $\text{Fe}_3$  possesses a doubly bridged Fe–Fe bond (unlike the common isomers of  $\text{Ru}_3(\text{CO})_{12}$  and  $\text{Os}_3(\text{CO})_{12}$ , which are unbridged).<sup>18</sup> The 2.14-Å bonds of  $\text{Fe}_3$  increase to 2.54 Å in the bridged edge and 2.68 Å in the unbridged edges of  $\text{Fe}_3(\text{CO})_{12}$ .<sup>22,23</sup> However, only a single bond exists between the metal atoms in the unbridged forms of  $\text{M}_3(\text{CO})_{12}$  as opposed to the double bond in  $\text{Fe}_2(\text{CO})_8$  (form U). It is possible that in producing  $\text{Fe}_3(\text{CO})_{12}$  from the  $\text{Fe}_3$  cluster precursor, it evolves through the unbridged intermediate with a structure like its Ru and Os analogues, but the barrier to rearrangement to the bridge form is lower than in the case of the  $\text{Fe}_2(\text{CO})_8$ .

In conclusion, we have shown that metal cluster complexes may be produced by co-depositing the ligand with size-selected metal cluster ions at low temperatures. As in previous cluster matrix depositions, we observe a low level of fragmentation, even though the mean kinetic energy exceeds the (per bond) bond energy by as much as a factor of 20. Likewise, the neutralization energy of the ions does not seem to lead to large-scale fragmentation. Finally, we show that direct cluster/ligand deposition can lead to novel complexes with structures differing from ones with the same metal nuclearity but produced by conventional means.

**Acknowledgment.** The authors gratefully acknowledge financial support from NSERC, the OLLRC, and CEMAID.

JA954243G

(19) Reinhold, J.; Hunstock, E.; Mealli, C. *New J. Chem.* **1994**, *18*, 465–471.

(20) Cotton, F. A.; Troup, J. M. *J. Chem. Soc., Dalton Trans.* **1974**, *8*, 800–802.

(21) Purdum, M.; Montano, P. A.; Shenoy, G. K.; Morrison, T. *Phys. Rev. B* **1982**, *25*, 4412–4419.

(22) Ballone, P.; Jones, R. O. *Chem. Phys. Lett.* **1995**, *233*, 632–638.

(23) Braga, D.; Grepioni, F.; Farrugia, L. J.; Johnson, B. F. G. *J. Chem. Soc. Dalton Trans.* **1994**, *20*, 2911–2918.